ON TRANSPARENT BOUNDARY CONDITIONS APPLICATION TO THE TROPOSPHERIC DUCTING PROPAGATION MODELING

Irina Sirkova
Department of Microwave Remote Sensing, Institute of electronics,
Bulgarian Academy of Sciences, 1784 Sofia, Bulgaria,
e-mail: iraids@yahoo.com,

Abstract

On the basis of the parabolic equation (PE) approximation to the wave equation in conjunction with the finite element (FE) method the applicability of recently reported in the literature nonlocal transparent boundary condition (NTBC) and the simpler local transparent boundary condition (LTBC) to the tropospheric ducting propagation (TDP) problems is studied and discussed. Ground-based, elevated ducts and cascades with smooth and piecewise linear modified refractivity profiles are used. Suggestions about the starting values for the transverse and propagation steps for both boundary conditions are made.

1. INTRODUCTION

The methods based on PE approach [1] to the Helmholtz wave equation are among the most widely used propagation modeling techniques for large classes of wave propagation problems [1]-[16]. This forward-scatter narrow-angle approximation has the advantage to be easily solved numerically through marching algorithms. PE primary drawback is that it neglects backscattering. In the tropospheric radio wave propagation prediction and assessment one is often interested in field variations over scales much larger then the wavelength and in these cases the forward-propagated field plays dominant role. The PE allows efficient and accurate numerical solutions for complicated refractive environment (including ducting), antenna patterns and underlying surface [7]-[16]. These reasons have turned the PE approach into the preferred technique for solving tropospheric propagation problems in a number of thoroughly validated and practically applied programs as PCPEM [9], TPEM [11], TEMPER [10], [13] (a representative list of the proposed and used models is given in [17]). Although considerable advance has been made in this field, some propagation effects and computational area problems still persist. Among them is the investigation of transparent boundary conditions that is related to the increasing of computational speed and the possibility to use propagation prediction models in operational situations. In this work the application of transparent boundary conditions to the TDP will be addressed.

Three main numerical techniques to solve the PE have become popular: the split-step Fourier algorithm [8]-[13], finite difference (FD) based algorithms [2], [3], [15] and algorithms using finite element (FE) method [4], [5], [16]. The split-step Fourier method has proven to be more stable numerically, thus allowing larger step sizes and shorter computational time, whereas FD and FE based schemes permit more flexibility in the implementation of various boundary conditions. Actually, the choice of the PE solution method depends strongly on the specific application. Whatever numerical technique to be chosen, as initial-value problem the PE requires specification of an initial field at a reference range (or altitude, if horizontal PE method will be applied, [14]) as well as boundary conditions in the other dimensions. The initial field is provided by the desired antenna pattern. The problem in the PE application to the TDP is that the natural (infinite) domain has to be truncated in height to the limited size of the computational window. To avoid the parasitic reflection from the artificial boundary back into the solution region the transformation of the zero-boundary condition at infinity to the boundary condition at the computational window upper boundary is required. (The problem with the parasitic reflection arises as well when the PE is applied for modeling structures permitting radiation losses, structures that scatter radiation and in some other cases [2].) The existing methods for solving this problem may be divided in two main groups [18], [19]. The first one (and most commonly used) consists in insertion of artificial absorbing layer adjacent to the concerned boundary. A small imaginary part is added to the refractive index near the extended computational window boundary so that the energy is absorbed and the reflection removed [9]. Or, viewing the discretized field as a sampled signal, the signal is “filtered” applying a suitable window in the extended region. In the TDP problems solution the filtering has been successfully used in [8], [12], [11] applying Hamming, Hanning and Tucky windows. More complicated algorithms for constructing the absorbing layer have also been reported [18]. If properly built, the artificial absorption procedure may be very accurate [2], [18]. Its drawback is the need to adjust the absorber parameters to each new problem. The absorbing layer increases additionally the integration domain that in the tropospheric case is inherently large enough, and, as a consequence, the computational time. Here arises the need of analytically found proper transparent boundary conditions that will insure as accurate as possible solution inside the computational window – this is the second group of solutions to the artificial boundary parasitic reflection problem. The

methods for constructing such boundary conditions give in general NTBC [3], [15], [19]-[23]. (A brief description of the derivation of the NTBC for some one, two and three-dimensional problems may be found in [23]). For the TDP problem the NTBC has been reported and successfully applied in [15] in conjunction with a FD based PE method. In [15] a NTBC accounting for the income of the energy through the upper window boundary has also been proposed thus permitting field assessment when the source is situated above the computational domain (which is not an exceptional case for the tropospheric propagation problems). The NTBCs minimize the magnitude of the reflected field and optimize the computational window size to the domain of interest (which has to include the essential tropospheric refractivity and terrain changes) but are quite complicated and require additional computational efforts. In some practical applications, for instance, radar performance assessment tools [10], propagation models are required to execute in real-time over large domain of interest with changeable parameters. For problems in which minimizing the reflected field is not of major importance and when limitations on computational cost are imposed some compromises in accuracy could be made applying simpler or more complex (modified) LTBC [2]-[5], [18]. In [24], the simpler LTBC [2], [5], firstly proposed and used in the integrated optics, was successfully applied to an important case of the TDP – the case of antenna submerged into a ground-based duct. This LTBC has the advantage to adjust the boundary correction term at every propagation step in straightforward manner thus providing rapid and accurate solution. A comparison between the reflectivity properties of the NTBC [15] and the simpler LTBC [5] applied for ground-based (evaporation) ducts propagation was made in [25].

In this paper, the applicability of the NTBC and the simpler LTBC to different TDP problems (ground-based, elevated ducts and cascades) is studied and discussed using the PE approximation in conjunction with the FE method. Suggestions about the starting values for the transverse and propagation steps for both boundary conditions are made.

2. THEORY

Assuming azimuthal symmetry, *exp(-iωt)* time dependence and earth-flattening approximation, the PE describing TDP can be written in the form (detailed derivation, validation and notes on the application of this equation for the case of tropospheric propagation may be found in [8], [9])

$$\frac{\partial^2 u(x,z)}{\partial z^2} + 2ik\frac{\partial u(x,z)}{\partial x} + k^2\left(m^2(z)-1\right)u(x,z) = 0, \tag{1}$$

where m stays for the modified tropospheric refractive index (here assumed not to vary in the propagation direction), k is the vacuum wave number, the rectangular coordinates z and x are thought of as altitude (z=0 at the Earth surface, x=0 at the antenna location) and range, respectively, and $u(x,z)$ is the reduced function, related to a field component [8], [9]. This equation holds for both, horizontal and vertical, polarizations the difference between them being contained in the boundary conditions at the Earth surface. In this work the Earth surface is considered smooth and perfectly conducting and the horizontal polarization is addressed.

To solve (1), the standard FE method using the weak Galërkin approximation [26] and the Crank-Nicholson algorithm has been applied. Description of this numerical procedure application to the TDP problem is reported in [16] and here only the final results of the NTBC and LTBC implementation in the FE scheme will be given.

2.1 NTBC implementation

The NTBC will be applied following [15] for the case when the initial field $u(0,z)$ is zero for z greater then Z_b, Z_b being the computational window upper boundary. This upper boundary must be chosen so that the computational window includes all refractivity and terrain particularities. The lower boundary is the Earth surface. The NTBC is taken in the form

$$\frac{\partial u(x,Z_b)}{\partial z} = \int_0^x \frac{\partial u}{\partial x}(t,Z_b)g_\alpha(x-t)dt \tag{2}$$

where

$$g_\alpha(x) = -\frac{i\alpha k}{2}\sum_{j=1}^{\infty}\frac{e^{p_j x}}{p_j} - \left(\alpha k^2\right)^{1/3} e^{2i\pi/3}\frac{Ai'(0)}{Ai(0)}, \tag{3}$$

$$p_j = \frac{\left(\alpha k^2\right)^{2/3}}{2k} e^{-i\pi/6} a_j, \tag{4}$$

a_j denotes the sequence of zeros of the Airy function Ai, [27], Ai' denotes the derivative, α (α>0) is the parameter from the modified refractive index definition above Z_b: $m^2(z)=1+\alpha(z-Z_b)$, see [15]. The NTBC defined by (2)-(4) involves the field and its derivatives along all the distance the field has already traveled. It is derived for linear change of m above Z_b and allows application for any refractive index structure below Z_b. In [15] the NTBC was validated for finite-difference PE implementation to the TDP problem. Here, discretizing (2)-(4) and applying the Crank-Nicholson algorithm for the propagation direction x, the following definitive matrix FE based equation with NTBC application is obtained from (1)

$$\left(A - \frac{\Delta x}{2}B\right)\{\gamma\}^n + \frac{u_b^n}{2}C = \left(A + \frac{\Delta x}{2}B\right)\{\gamma\}^{n-1} - \frac{u_b^{n-1}}{2}\tilde{C} - D_{n-2} + u_b^0 C_0^n \tag{5}$$

where the superscript n denotes the quantities related to the nth propagation step, superscript n-1 - the quantities related to the (n-1)th propagation step, the subscript b indicates that the quantity is taken at Z_b, the term D_{n-2} accumulates the influence of the preceding steps. The coefficients C and the term D_{n-2} are as follows

$$C = \frac{i\alpha k}{2}\left(\frac{(2k)^2 e^{i\pi/3}}{\left(\alpha k^2\right)^{4/3}}\left(\frac{Ai'(0)}{Ai(0)}\right)^2 - \sum_{j=1}^{\infty}\frac{e^{p_j\Delta x}}{p_j^2}\right) - F, \tag{6}$$

$$\tilde{C} = \frac{i\alpha k}{2}\left(\sum_{j=1}^{\infty}\frac{3e^{p_j\Delta x}-2e^{2p_j\Delta x}}{p_j^2}-\frac{(2k)^2 e^{i\pi/3}}{\left(\alpha k^2\right)^{4/3}}\left(\frac{Ai'(0)}{Ai(0)}\right)^2\right)-F, \tag{7}$$

$$D_{n-2} = \sum_{l=1}^{n-2}u_b^l\,\frac{i\alpha k}{2}\sum_{j=1}^{\infty}\frac{e^{p_j(n-l)\Delta x}}{p_j^2}\left(e^{-p_j\Delta x}-1\right)\left(e^{p_j\Delta x}-1\right), \tag{8}$$

$$C_0^n = \frac{i\alpha k}{2}\sum_{j=1}^{\infty}\frac{e^{p_j n\Delta x}}{p_j^2}\left(e^{-p_j\Delta x}-1\right)-F \tag{9}$$

where

$$F = \left(\alpha k^2\right)^{1/3} e^{2i\pi/3}\,\frac{Ai'(0)}{Ai(0)}\Delta x. \tag{10}$$

The numerical problem concerning the convergence of these coefficients (notably for $\Delta x \to 0$) has been solved using the suggestion made in [15]. In (5) the vector $\{\gamma\}$ and the expanded matrices A and $B=L-k^2M$ are given by

$$\{\gamma\} = [\gamma_1\gamma_2...\gamma_N]^T, \tag{11}$$

$$[A]_{ij}^e = 2ik\int_e \Psi_i\Psi_j dz, \tag{12}$$

$$[L]_{ij}^e = \int_e \frac{d\Psi_i}{dz}\frac{d\Psi_j}{dz}dz, \tag{13}$$

$$[M]_{ij}^e = \left(m^2(z)-1\right)\int_e \Psi_i\Psi_j dz. \tag{14}$$

In (11)-(14) N is the total number of nodes in the problem cross-section, γ_j is the value of u at node j, Ψ_j are the basis functions (linear polynomials) defined over an element

e (the elements are line segments), [16], [26], *T* denotes a transpose. In (14) $m^2(z)$ is assumed constant within the element.

An appropriate boundary condition was proposed in [15] as well for the case of source situated above the computational window. Such kind of problems may arise in the case of plane or satellite-earth communications. If only the field close to the earth surface is of interest, the reduction of the computational window cross-section to a height below the source height Z_a could speed up considerably the computation. Here a brief description of the incoming energy term is given following [15] and the FE computational scheme accounting for it is provided.

With inclusion of the incoming energy term *I(x)*, the NTBC has the form:

$$\frac{\partial u}{\partial z}(x, Z_b) = \int_0^x \frac{\partial u}{\partial t}(t, Z_b) g_\alpha (x-t) dt + I(x), \tag{15}$$

where *I(x)* is given by:

$$I(x) = \frac{\partial v}{\partial z}(x, Z_b) - \int_0^x \frac{\partial v}{\partial x}(t, Z_b) g_\alpha (x-t) dt \tag{16}$$

and g_α is the same as in (3). Now the problem is to find the auxiliary function *v(x,z)* which is a solution of the PE in the domain $z \geq Z_b$ with $v(0,z)=u(0,z)\neq 0$ for $z \geq Z_b$. As was shown in [15], for linear medium above Z_b and source at height Z_a with aperture function (corresponding to a Gaussian beam pattern) of the form:

$$u(0,z) = \exp(-A(z-Z_a)^2), \quad A = \frac{-k^2\theta_0^2}{4\log(0.707)} \tag{17}$$

where θ_0 is the half-power beamwidth angle, the function *v(x,z)* is:

$$v(x,z) = \sqrt{\frac{k}{k+2iAx}} \exp\left[\frac{ik\alpha x(z-Z_b)}{2} - \frac{2}{3} ik\alpha^2 x^3 - kA\frac{\left(Z_a - z + \alpha x^2/4\right)^2}{k+2iAx}\right]. \tag{18}$$

The inclusion of the incoming term in the computational scheme requires the following expression to be added to the right-hand side of (5)

$$-\frac{\Delta x}{2}\left[\frac{\partial v(x_{n-1},Z_b)}{\partial z}+\frac{\partial v(x_n,Z_b)}{\partial z}\right]+\frac{\Delta x}{2}\left[2\sum_{l=0}^{n-2}\frac{\partial v\left(\frac{x_l+x_{l+1}}{2}\right)}{\partial x}C_l+\frac{\partial v\left(n\Delta x-\frac{\Delta x}{2}\right)}{\partial x}C\right] \quad (19)$$

where the derivatives $\partial v/\partial z$ and $\partial v/\partial x$ are obtained from (18), the coefficient C is given by (6) and C_l is

$$C_l=\frac{i\alpha k}{2}\sum_{j=1}^{\infty}\frac{e^{p_j(n-l)\Delta x}\left(e^{-p_j\Delta x}-1\right)}{p_j^2}-F\,. \quad (20)$$

In (20) p_j and F are the same as given in (4) and (10), respectively.

The above described NTBC provides correct solution to the radiation boundary condition problem but its application is not a straightforward task at all. On the other hand, the rays corresponding to the PE (1) bend upward and leave the upper boundary rapidly, i. e. the boundary has short “memory” and only the nearest neighbor points contribute to the boundary condition at the current point. The attempts to simplify the NTBC relying on this property (for instance, by presenting the discretized (2) in the form of inhomogeneous impedance boundary condition, i. e.

$$\frac{\partial u_b^n}{\partial z}=\frac{u_b^n}{\Delta x}C+B,$$

$$B=\sum_{l=1}^{n-1}\frac{u_b^l}{\Delta x}\tilde{C}-\frac{u_b^0}{\Delta x}C_0^n,\ \tilde{C}=\frac{i\alpha k}{2}\sum_{j=1}^{\infty}\frac{e^{p_j(n-l)\Delta x}}{p_j^2}\left(e^{-p_j\Delta x}-1\right)\left(e^{p_j\Delta x}-1\right),\ C \text{ and } C_0^n \text{ as given in (6) and (9), respectively,}$$

with subsequent preservation of C and omission of the “tail” B when the derivative is introduced in the computational scheme) have not given good results because they remain constant for every cross-section. The above observations gave reasons to try the LTBC [2]-[5] application to the TDP problem.

2.2 LTBC implementation

The introduction to the LTBC will be made following [4]. The assumption that the field in the vicinity of the computational window boundary Z_b consists of an outgoing plane wave and does not include any reflected wave leads to the field in the form

$$u(x,z) = c\exp(\alpha x + \beta z). \tag{21}$$

Equation (21) provides the following relation between the field and its z-derivative

$$\left(\frac{\partial u}{\partial z}\right) = \beta u\,. \tag{22}$$

As no reflection exists in the description of the field given by (21), equation (22) represents (local) transparent boundary condition [2]-[5]. The simplest way to obtain the unknown wave number β in the z direction is the following: at the step x^n it is determined using the former-step field distribution. Thus for β at the upper boundary of the computational window we obtain from (22)

$$\beta_N^n = \frac{1}{\Delta z}\log\left(\frac{u_N^{n-1}}{u_{N-1}^{n-1}}\right). \tag{23}$$

The final matrix FE based equation with LTBC application is

$$\left(A - \frac{\Delta x}{2}B\right)\{\gamma\}^{(n)} = \left(A + \frac{\Delta x}{2}B\right)\{\gamma\}^{(n-1)} \tag{24}$$

where $\{\gamma\}$ and the matrices A and $B=L-k^2M+K$ are as given above, (11) – (14), and matrix K is

$$[K]=\begin{bmatrix} 0 & 0 & . & . & 0 \\ 0 & 0 & . & . & 0 \\ . & & & & . \\ . & & & & . \\ 0 & 0 & . & . & K_N \end{bmatrix}. \qquad . \tag{25}$$

The matrix K contains the simplest form of the LTBC as described in [2], [5]. The term K_N is given by (23) and renewed at every propagation step. A correction to the imaginary part of this term has to be made (if necessary) at every step in order to ensure the radiation outflow. A more refined way of determination of β is introduced in [2]. For the case of ground-based duct the LTBC scheme (23)-(25) was applied and validated in [24].

3. RESULTS AND DISCUTION

The LTBC and NTBC have been applied to ground-based, elevated and the combination of ground-based and elevated ducts for different antenna heights. Two kinds of modified refractivity $M(z)=10^6(m(z)-1)$ profiles have been used: piecewise linear and smooth continuous profile. This is done in order to avoid any kind of "privileges" of the linear profiles and to use more realistic refractivity. A suitable smooth profile, allowing the modeling of a simple elevated or ground-based duct as well as the synthesis of more complicated profiles, was suggested in [28], [29]

$$M(z)=\alpha z+\frac{\Delta N}{\pi}\arctan\left[\frac{12.63(z-z_0)}{\Delta z}\right] \tag{26}$$

where ΔN is the total change in the refractivity N (N is related to the modified refractivity M through $M=N+10^6 z/a_e$, where a_e is the Earth radius), z_0 is the height at the center of the change ΔN, Δz is the height range between points at which the change has reached 90 percent of its final value and α represents the basic gradient for the standard atmosphere (i. e. α=.118 N units/m). The parameters of the used profiles are presented in Table I (taken from [28]) and Table II (profile a taken from [15]). The initial field is provided by a Caussian beam antenna with half-power beamwidth

of 1°, no tilt of the beam and transmitting frequency of 10 GHz, see (17). The results are presented in the form of path loss (PL, in dB)

$$PL = 20\log\left(\frac{4\pi x}{\lambda}\right) - PF \tag{27}$$

where λ is the free-space wavelength and PF is the pattern propagation factor as defined in [30] (at a given point PF provides the excess signal strength (under the specified refractive conditions) over free-space without accounting for atmospheric absorption but including antenna pattern). For all figures, except Fig. 8 and Fig. 24, one and the same Z_b=500 m has been used. This computational window upper boundary insures proper LTBC application for all reported cases. The computational steps are chosen according to [25].

Table I Smooth modified refractivity profiles

Profile	ΔN	Δz	z_0
a	-20	100	175
b	-50	100	-10
c	-20	150	150
d	7	200	75

Table II Piecewise linear modified refractivity profiles

Profile	Height (m)	M (M-units)
a	0	5
	50	0
	1050	118
b	0	5
	50	0
	200	17.7
	300	2.7
	1300	120.7

Figs. 1 and 2 show PL (with LTBC and NTBC application, respectively) for an elevated duct with thickness Z_d=144 m formed by the smooth *M* provided by profile *a* from Table I with antenna embedded inside the duct. The combination of profile *b* and *c* from Table I gives an elevated duct with Z_d=175 m that absorbs a ground-based Z_d=22.5 m duct. For this profile Figs. 3 and 5 show PL with LTBC application for antenna height Z_a=10 m (inside the lower duct) and Z_a=100 m (between the two inversions), respectively. The analogous PL but with NTBC application are shown on Figs. 4 and 6. Figs. 7 and 8 are obtained applying the bilinear profile *a* from Table II (ground-base duct, Z_d=50 m) for elevated antenna with Z_a=250 m. For fig. 7 LTBC computation with Z_b=500 m has been cut at z=50 m. Fig. 8 is obtained applying the NTBC scheme (5) with the incoming energy term (19) at Z_b=50 m. The combination of profile *b*, *c* and *d* from Table I gives a cascade of two inversions, the first one has Z_d=22.5 m and the second (elevated) has Z_d=106 m.

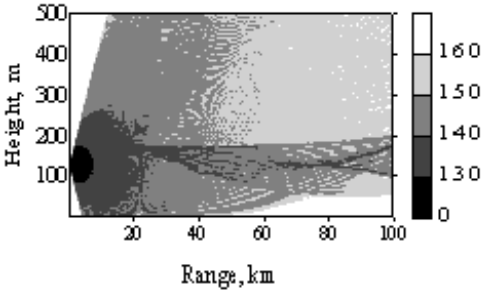

Fig. 1 PL for profile a from Table I, Zd between 50 and 194 m, Za=125 m, LTBC at Zb=500 m.

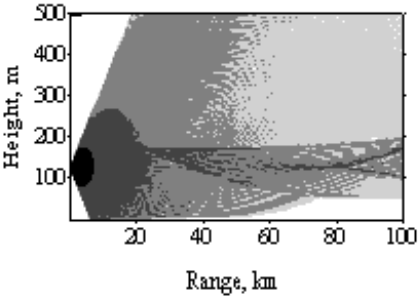

Fig. 2 PL for profile a from Table I, Zd between 50 and 194 m, Za=125 m, NTBC at Zb=500 m.

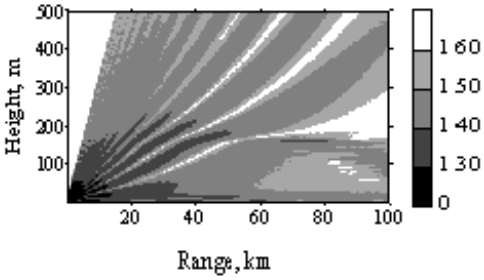

Fig. 3 PL for profile b+c from Table I, the upper duct (0-175 m) absorbs the lower one (0-22.5 m), Za=10 m, LTBC at Zb=500 m.

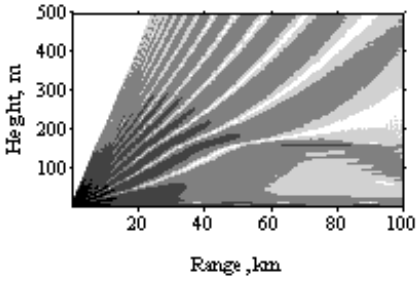

Fig. 4 PL for profile b+c from Table I, the upper duct (0-175 m) absorbs the lower one (0-22.5 m), Za=10 m, NTBC at Zb=500 m.

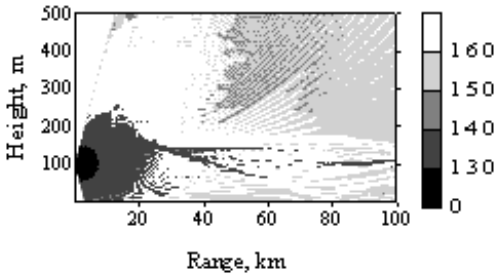

Fig. 5 PL for profile b+c from Table I, the upper duct (0-175 m) absorbs the lower one (0-22.5 m), Za=100 m, LTBC at Zb=500 m.

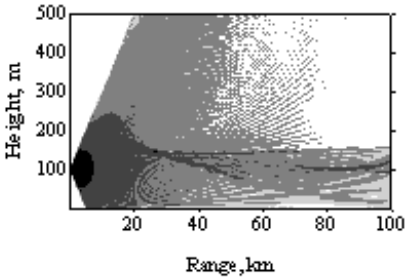

Fig. 6 PL for profile b+c from Table I, the upper duct (0-175 m) absorbs the lower one (0-22.5 m), Za=100 m, NTBC at Zb=500 m.

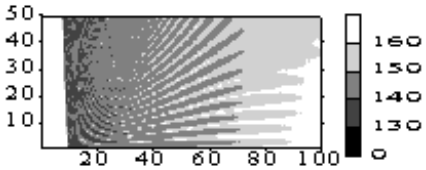

Fig.7 PL for profile a from Table II, Za=250, LTBC at Zb=500 m.

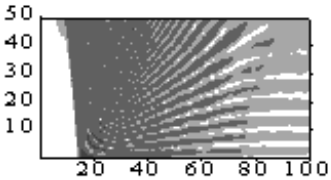

Fig.8 PL for profile a from Table II, Za=250, NTBC at Zb=50 m, incoming energy scheme.

Figs. 9, 11, 13 and 15 show PL for this profile with LTBC application and Z_a inside the lower inversion, between the two inversions, inside the upper one and above the inversions, respectively. The same but with NTBC application is shown on Figs. 10,12,14 and 16. The piecewise linear profile *b* from Table II gives a cascade with

upper Z_d=226 m and lower Z_d=50 m. Figs. 17,19, 21 show PL for this profile and different antenna heights with LTBC application, whereas on Figs. 18, 20 and 22 PL for the same cases with NTBC application are plotted.

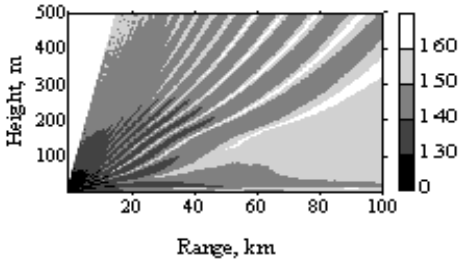

Fig. 9 PL for profile b+c+d from Table I, upper duct between 66 and 172 m, lower duct Zd=22.5 m, Za=15 m, LTBC at Zb=500 m.

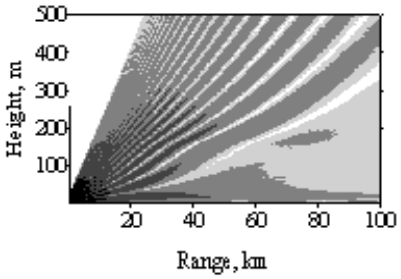

Fig. 10 PL for profile b+c+d from Table I, upper duct between 66 and 172 m, lower duct Zd=22.5 m, Za=15 m, NTBC at Zb=500 m.

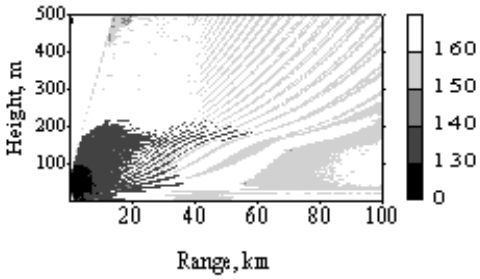

Fig. 11 PL for profile b+c+d from Table I, upper duct between 66 and 172 m, lower duct Zd=22.5 m, Za=50 m, LTBC at Zb=500 m.

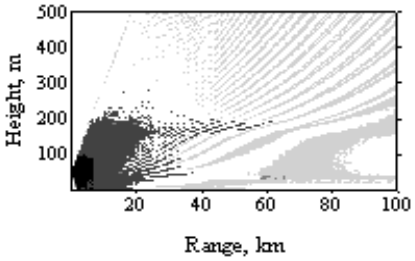

Fig. 12 PL for profile b+c+d from Table I, upper duct between 66 and 172 m, lower duct Zd=22.5 m, Za=50 m, NTBC at Zb=500 m.

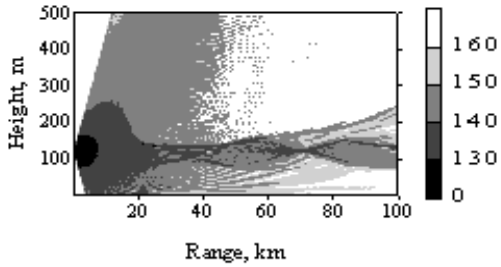

Fig. 13 PL for profile b+c+d from Table I, upper duct between 66 and 172 m, lower duct Zd=22.5 m, Za=120 m, LTBC at Zb=500 m.

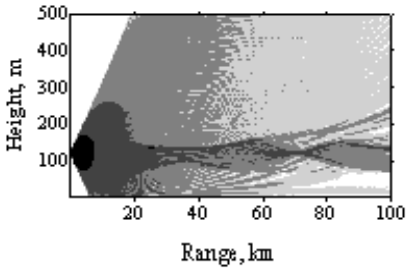

Fig. 14 PL for profile b+c+d from Table I, upper duct between 66 and 172 m, lower duct Zd=22.5 m, Za=120 m, NTBC at Zb=500 m.

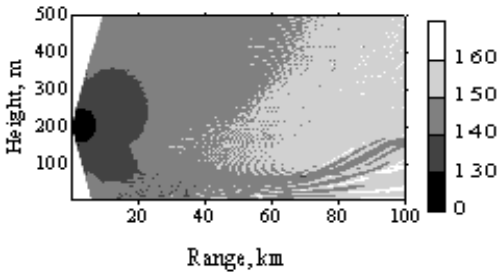

Fig. 15 PL for profile b+c+d from Table I, upper duct between 66 and 172 m, lower duct Zd=22.5 m, Za=200 m, LTBC at Zb=500 m.

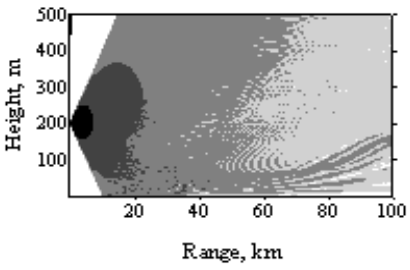

Fig. 16 PL for profile b+c+d from Table I, upper duct between 66 and 172 m, lower duct Zd=22.5 m, Za=200 m, NTBC at Zb=500 m.

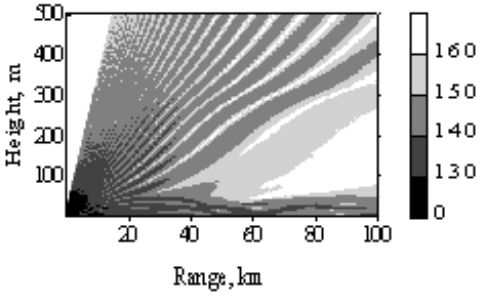

Fig. 17 PL for profile b from Table II, upper duct between 74 and 300 m, lower duct Zd=50 m, Za=20 m, LTBC at Zb=500 m.

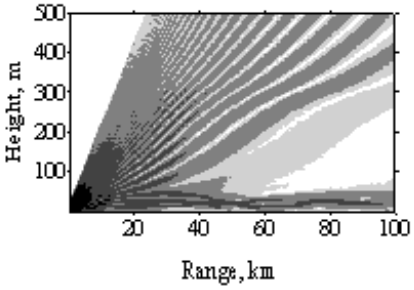

Fig. 18 PL for profile b from Table II, upper duct between 74 and 300 m, lower duct Zd=50 m, Za=20 m, NTBC at Zb=500 m.

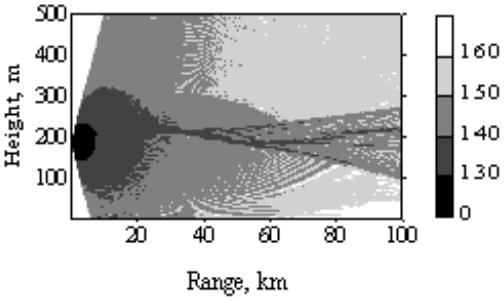

Fig. 19 PL for profile b from Table II, upper duct between 74 and 300 m, lower duct Zd=50 m, Za=185 m, LTBC at Zb=500 m.

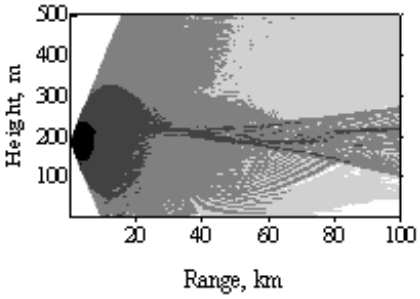

Fig. 20 PL for profile b from Table II, upper duct between 74 and 300 m, lower duct Zd=50 m, Za=185 m, NTBC at Zb=500 m.

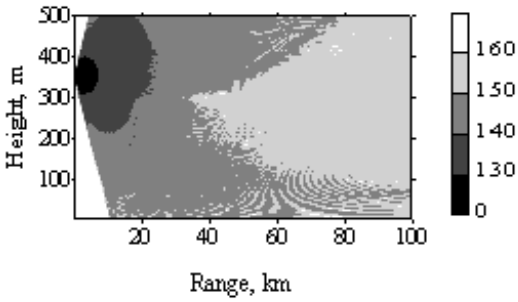

Fig. 21 PL for profile b from Table II, upper duct between 74 and 300 m, lower duct Zd=50 m, Za=350 m, LTBC at Zb=500 m.

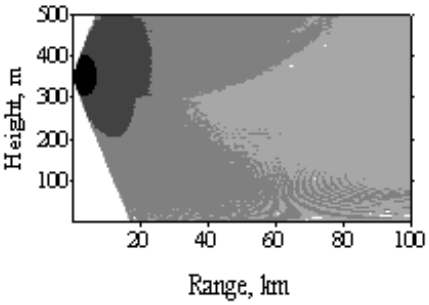

Fig. 22 PL for profile b from Table II, upper duct between 74 and 300 m, lower duct Zd=50 m, Za=350 m, NTBC at Zb=500 m.

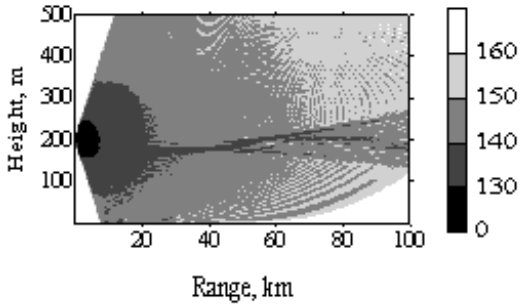

Fig. 23 PL for elevated duct between 100 and 300 m, trapping layer between 185 and 300 m with strength 10 M units, Za=200 m, LTBC at Zb=500 m.

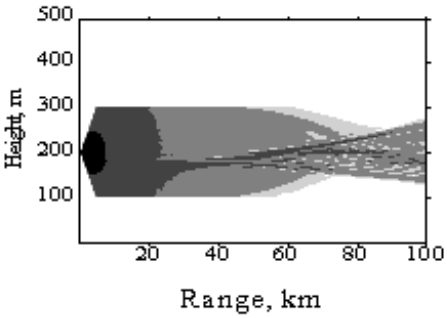

Fig. 24 PL for elevated duct between 100 and 300 m, trapping layer between 185 and 300 m with strength 10 M units, Za=200 m, NTBC at 100 and 300 m.

From the above examples it is clear that the LTBC presents results close enough to those given by the NTBC. To correctly implement the LTBC, Z_b must be chosen in the region where the field immediately below Z_b will have the same behavior as above it, i. e. the behavior of an outgoing wave. For every specific M profile and antenna type and location it is a matter of adjustment to find this region, but it can not be just above the duct. For the NTBC Z_b could be equal to the upper duct boundary in both, $u(0,z)=0$ for $z \geq Z_b$ and $u(0,z) \neq 0$ for $z \geq Z_b$, cases. For a given TDP case the LTBC requests greater value for Z_b but even with this Z_b (taken above the ducting region with a great reserve) the LTBC provides faster solution than the NTBC. The straightforward manner the boundary correction term is introduced and renewed at every step explains this speed but is not the only reason. As was reported in [3] and [25], in the LTBC application the smallest steps do not assure the best results because the reflectivity presents clearly pronounced minimum in respect of the transverse step for a fixed propagation step. For the above made calculations transverse step Δz=.5 m for the LTBC and Δz=.25 m for the NTBC application have been used for all cases with a propagation step Δx=20 m [25], the LTBC allowing propagation step up to 100 m. These steps could be recommended as starting steps for the LTBC and NTBC in their TDP application. Thus, for the LTBC there is not a need of refinement of the scheme, whereas the NLBC works as better as smaller are the steps.

It is tempting to apply the LTBC and NTBC to the lower computational window boundary if one is interested only in the field inside an elevated region. Below this boundary the field does not have the character of an outgoing wave (a comment about this case may be found in [23]). Nevertheless, it is possible to implement transparent boundary condition to the lower boundary if this one coincides with the lower boundary of a strong elevated duct and the source is situated within the duct. In this case the energy coming back to the computational domain from below will be lost but the essential distribution of the field inside the duct will be preserved. This is illustrated on Figs. 23 and 24 for a profile with trapping layer between 185 and 300 m giving duct between 100 and 300 m. Fig. 23 is obtained applying LTBC at Z_b=500 m whereas Fig. 24 shows the result for the NTBC application to the lower and upper duct boundaries.

On some pictures with NTBC application (Fig. 6, Fig. 12) one may notice reflection that is not expected to appear. The coincidence between Fig. 7 and Fig. 8 is not perfect, see also the lower part of Fig. 3 from [15] where the same example is reported. A possible explanation, especially for Fig. 8, may be the improper step sizes choice. More generally, this discrepancy may be due to the manner the x-derivative was introduced in the NTBC scheme. The discretization of (2) requires splitting of the integral from zero to x into integrals over subintervals $[x_n, x_{n+1}]$. Over each subinterval $[x_n, x_{n+1}]$ $\partial u/\partial x$ term in (2) is treated as a constant while g_α is integrated exactly. The results could be improved as well applying more sophisticated FE scheme but this will increase the computational time.

4. CONCLUSION

Recently reported in the literature NTBC [15] and the simpler LTBC [2]-[5] have been applied to different TDP problems with smooth and piecewise linear refractivity profiles using the PE approximation in conjunction with the FE method. Suggestions are made about the starting values of the transverse and propagation step sizes for both LTBC and NTBC. On the basis of comparisons between the two transparent boundary conditions it is considered that the LTBC may be applied in all TDP cases taking advantage of its simplicity and lower time consummation. It is quite clear that this simple technique may offer the possibility of real-time electromagnetic field prediction under operational situations.

ACKNOWLEDGMENT: This work was initiated and partially done under project No 96/09971-1 of FAPESP (Research Foundation of the State of Sao Paulo). The author wishes to thank also Dr. Hugo E. Hernandez-Figueroa for his support.

REFERENCES

[1] F. D. Tappert, “The parabolic approximation method”, in *Wave Propagation and Underwater Acoustics*. J. B. Keller and J. S. Papadakis (Eds.), New York: Springer-Verlag, 1977.

[2] G. R. Hadley, “Transparent boundary condition for the beam propagation method”, *J. Quant. Elect.*, vol. 28, no. 1, pp. 363-370, Jan. 1992.

[3] G. H. Song, "Transparent boundary condition for beam-propagation analysis from the Green´s function method", *J. Opt. Soc. Amer. A*, vol. 10, no. 5, pp. 896-904, May 1993.

[4] Y. Arai, A. Maruta and M. Matsuhara, "Transparent boundary for the finite-element beam propagation method", *Opt. Lett.*, vol. 18, no. 10, pp. 765-766, May 1993.

[5] Y. Tsuji and M. Koshiba, "A finite element beam propagation method for strongly guiding and longitudinally varying optical waveguides", *J. Lightwave Technol.*, vol. 14, no. 2, pp. 217-222, Feb. 1996.

[6] A. A. Zaporozhets and M. F. Levy, "Modeling of radiowave propagation in urban environment with parabolic equation method", *Electron. Lett.*, vol. 32, no. 17, pp. 1615-1616, Aug. 1996.

[7] N. Douchin, S. Bolioli, F. Christophe and P. Combes, "Theoretical study of the evaporation duct effects on the satellite-to ship radio links near the horizon", *IEE Proc. F,* vol. 141, no. 4, pp. 272-278, Aug. 1994.

[8] J. R. Kuttler and G. D. Dockery, "Theoretical description of the parabolic approximation/Fourier split-step method of representing electromagnetic propagation in the troposphere", *Radio Sci.*, vol. 26, pp. 381-393, March-Apr. 1991.

[9] K. G. Craig and M. F. Levy, "Parabolic equation modeling of the effects of multipath and ducting on radar systems", *IEE Proc. F***,** vol. 138, no. 2, pp.153-162, Apr. 1991.

[10] G. D. Dockery, "Development and use of electromagnetic parabolic equation propagation models for U. S. navy applications", *Johns Hopkins APL Technical Digest,* vol. 19, no. 3, pp. 283-292, 1998.

[11] A. Barrios, "A terrain parabolic equation model for propagation in the troposphere", *IEEE Trans, Antennas Propagat.*, vol. 42, no. 1, pp. 90-98, Jan. 1994.

[12] R. Janaswamy, "A curvilinear coordinate-based split-step parabolic equation method for propagation prediction over terrain", *IEEE Trans. Antennas Propagat.*, vol. 46, no. 7, pp. 1089-1097, July 1998.

[13] D. J. Donohue and J. R. Kuttler, "Modeling radar propagation over terrain", *Johns Hopkins APL Technical Digest*, vol. 18, no. 2, pp. 279-287, 1997.

[14] M. F. Levy, “Horizontal parabolic equation solution of radiowave propagation problems on large domains”, *IEEE Trans. Antennas Propagat.*, vol. 43, no. 2, pp. 137-144, Feb. 1995.

[15] M. F. Levy, “Transparent boundary conditions for parabolic equation solutions of radiowave propagation problems”, *IEEE Trans. Antennas Propagat.*, vol. 45, no. 1, pp. 66-72, Jan. 1997.

[16] H. E. Hernandez-Figueroa and I. Sirkova, “Finite elements application to the tropospheric ducting problem”, in *Proc. III Brazilian Meeting on Software and Measurements in Microwaves and Optoelectronics,* Campinas, SP, Brazil, Dec. 1997, pp. 58-61.

[17] R. H. Ott, “A line-of-site propagation model for calculating atmospheric, sea, terrain multipath and clutter at microwave frequencies”, *Radio Sci.*, vol. 32, no. 2, pp. 369-386, March-April 1997.

[18] D. Yevick, J. Yu and Y. Yayon, “Optimal absorbing boundary conditions”, *J. Opt. Soc. Amer. A*, vol. 12, no. 1, pp. 107-110, Jan. 1995.

[19] F. Schmidt and D. Yevick, “Discrete transparent boundary conditions for Schrödinger-type equations”, *Preprint SC* 96-17, pp. 1-20, May 1996.

[20] S. W. Marcus, “A hybrid (finite difference-surface Green’s function) method for computing transmission losses in an inhomogeneous atmosphere over irregular terrain”, *IEEE Trans. Antennas Propagat.*, vol. 40, no. 12, pp. 1451-1458, Dec 1992.

[21] R. A. Dalrymple and P. A. Martin, “Perfect boundary conditions for parabolic water-wave models”, in *Proc. R. Soc. A,* London, U.K., vol. 437, pp. 41-54, Apr. 1992.

[22] J. S. Papadakis, “Exact, nonreflecting boundary conditions for parabolic-type approximation to underwater acoustics”, *J. Comput. Acoust.,* vol. 2, no. 2, pp. 83-98, Fev. 1994.

[23] A. V. Popov, “Accurate modeling of transparent boundaries in quasi-optics”, *Radio Sci.*, vol. 31, no. 6, pp. 1781-1790, Nov.-Dec. 1996.

[24] I. Sirkova and H. E. Hernandez-Figueroa, “Local Transparent Boundary Condition Applied to the Modeling of Tropospheric Ducting Propagation”, *Microw. Opt. Technol. Lett.,* vol. 21, no. 5, pp. 343-346, June 1999.

[25] I. Sirkova, "Comparison between a local and a nonlocal transparent boundary conditions applied to the tropospheric ducting propagation problem", to appear in *Microw. Opt. Technol. Lett.*, vol. 25, no. 1, 2000.

[26] J. Jin, *The Finite Element Method in Electromagnetics.* New York: Wiley-Interscience Publication, 1993.

[27] M. Abramowitz and I. Stegun, *Handbook of Mathematical Functions.* New York: Dover Publications Inc., 1972.

[28] A. R. Webster, "Raypath parameters in tropospheric multipath propagation", *IEEE Trans. Antennas Propagat.*, vol. 30, no. 4, pp. 796-800, July 1982.

[29] D. Rana, A. R. Webster and M. Sylvain, "Statistical characterization of line-of-sight microwave link", *Radio Sci.*, vol. 27, no. 6, pp. 783-796, Nov.-Dec. 1992.

[30] D. E. Kerr (Ed.), *Propagation of short radiowaves*. London: P. Peregrinus, 1987.